

# Identifying the quantum correlations in light-harvesting complexes

Kamil Brádler and Mark M. Wilde

*School of Computer Science, McGill University, Montreal, Quebec, Canada H3A 2A7*

Sai Vinjanampathy

*Department of Physics and Astronomy, Louisiana State University, Baton Rouge, Louisiana 70803, USA*

Dmitry B. Uskov

*Department of Physics and Engineering Physics, Tulane University, New Orleans, Louisiana 70118, USA; and**Department of Mathematics and Natural Sciences, Brescia University, Owensboro, Kentucky 42301, USA*

(Received 10 September 2010; published 13 December 2010)

One of the major efforts in the quantum biological program is to subject biological systems to standard tests or measures of quantumness. These tests and measures should elucidate whether nontrivial quantum effects may be present in biological systems. Two such measures of quantum correlations are the quantum discord and the relative entropy of entanglement. Here, we show that the relative entropy of entanglement admits a simple analytic form when dynamics and accessible degrees of freedom are restricted to a zero- and single-excitation subspace. We also simulate and calculate the amount of quantum discord that is present in the Fenna-Matthews-Olson protein complex during the transfer of an excitation from a chlorosome antenna to a reaction center. We find that the single-excitation quantum discord and single-excitation relative entropy of entanglement are equal for all of our numerical simulations, but a proof of their general equality for this setting evades us for now. Also, some of our simulations demonstrate that the relative entropy of entanglement without the single-excitation restriction is much lower than the quantum discord. The first picosecond of dynamics is the relevant time scale for the transfer of the excitation, according to some sources in the literature. Our simulation results indicate that quantum correlations contribute a significant fraction of the total correlation during this first picosecond in many cases, at both cryogenic and physiological temperatures.

DOI: [10.1103/PhysRevA.82.062310](https://doi.org/10.1103/PhysRevA.82.062310)

PACS number(s): 03.67.Mn, 03.65.Yz, 82.39.Jn

## I. INTRODUCTION

Quantum biology aims to understand if, how, and why biological systems exploit quantum-mechanical effects for their functionality or for an evolutionary advantage [1–4]. Exemplary biological systems that may exploit quantum effects vary from photosynthetic light-harvesting complexes [5], to the avian compass for bird navigation [6], to the olfactory system [7]. Ongoing theoretical research indicates that light-harvesting complexes exploit an environment-assisted quantum-walk-like effect to enhance energy transport [8–11], the avian compass exploits a radical ion-pair mechanism for increased sensitivity of the earth’s geomagnetic field [12–14], and the olfactory system may exploit phonon-assisted tunneling for enhanced detection of smell [7].

Light-harvesting complexes seem particularly suitable as biological systems to harness quantum-mechanical effects. Their length scales and energy scales are on the order where we would expect quantum-mechanical laws to apply [15], but what remains less clear is whether they can still harness quantum effects such as entanglement even at physiological temperature. A recent numerical study addresses this question by showing that light-harvesting complexes could demonstrate stronger-than-classical *temporal* correlations, even at physiological temperature [16]. However, it remains an open task to devise and conduct a realistic experimental protocol that demonstrates an irrevocable test of nonclassical temporal correlations for light-harvesting complexes.

The aim of the study in Ref. [16], as well as that in Refs. [17,18], is to address one of the important “quantum

biological questions”: *Does the biological system exhibit “quantumness” according to a standard test or measure?* Theoretical machinery from quantum information science [19], developed specifically for understanding quantum computational and communication devices, should be of immense utility in answering this question. Several articles have already begun exploiting such tools. Reference [16] exploits the Leggett-Garg test of nonclassicality [20] to suggest that light-harvesting complexes might exhibit stronger-than-classical temporal correlations, while Refs. [17,18] utilize standard entanglement-based measures of quantum correlations [21–23] to suggest that they might exhibit stronger-than-classical spatial correlations. Such standard measures of quantum behavior are more convincing than, say, a claim that wavelike motion in population elements of a density matrix is a signature of quantumness [24].

The studies in Refs. [17,18] both suggest that it might be possible to observe spatial quantum correlations in the Fenna-Matthews-Olson (FMO) light-harvesting protein complex, but the quantum correlation measures exploited there, such as concurrence [25], the measure based on the global relative entropy of entanglement [23], and logarithmic negativity [26], might not capture all of the spatial quantum correlations that are present in a given quantum system. For example, consider a bipartite quantum system in the state

$$\frac{1}{2} |0\rangle \langle 0|^A \otimes |+\rangle \langle +|^B + \frac{1}{2} |-\rangle \langle -|^A \otimes |1\rangle \langle 1|^B, \quad (1)$$

where  $|\pm\rangle \equiv (|0\rangle \pm |1\rangle)/\sqrt{2}$ , Alice possesses the system  $A$ , and Bob possesses the system  $B$ . The state in (1) is a separable

state [27], meaning that Alice and Bob can prepare it by means of local quantum operations and classical communication. Yet, it is fundamentally nonclassical because the states  $|0\rangle$  and  $|-\rangle$  on Alice's local system or  $|1\rangle$  and  $|+\rangle$  on Bob's local system are indistinguishable from one another (they are nonorthogonal). It could be possible for two bacteriochlorophyll sites of a light-harvesting complex to admit a state of the above class or a mixture of such states, but the quantum correlation measures mentioned above all vanish for such a separable state, despite its status as a fundamentally nonclassical state. Thus, these measures might not capture the full quantumness that might be present in a light-harvesting complex.

A different measure of quantum correlations, known as the quantum discord [28,29], captures all correlations in a quantum state that are nonclassical. The discord is a measure of the total correlations present in a shared quantum state, reduced by the classical correlations obtainable when one party performs a local measurement. For example, the state in (1) registers a nonvanishing quantum discord and therefore possesses nonclassical correlations according to this measure, even though it does not violate a Bell inequality [30] due to it being a separable state. Other examples demonstrate that the quantum discord in a quantum system can remain positive even if the entanglement vanishes after a finite time [31]. States that register nonvanishing discord can lead to exponential speedups [32,33] in a quantum computational model known as the "one-clean-qubit model" [34], where the only requirement for a speedup is access to a single qubit in a pure state. Although it is unlikely that a light-harvesting complex could be performing exotic quantum computational speedups of the aforementioned nature or in the standard way [35], one cannot rule out the possibility that a light-harvesting complex exhibiting nonvanishing discord could be exploiting quantumness of this form for enhanced energy transport.

In this paper, we systematically study the presence of quantum correlations in the FMO light-harvesting complex, at both cryogenic and physiological temperatures. Our first contribution is a simple formula for computing the relative entropy of entanglement [36] when a light-harvesting complex evolves according to the open quantum system model well studied in the quantum biological literature [9,10]. This formula assumes that dynamics are restricted to a zero- and single-excitation subspace, and it reduces the *a priori* computationally intensive optimization task for computing the single-excitation relative entropy of entanglement to a simple calculation with quantum entropies. These results for the single-excitation relative entropy of entanglement generalize those of Sarovar *et al.* in Ref. [17] for the global relative entropy of entanglement. We then calculate the single-excitation quantum discord for several phenomenologically motivated "bipartite cuts" of the FMO protein complex and find that it is equivalent to the single-excitation relative entropy of entanglement in all cases presented here. These results demonstrate that quantum correlations contribute a significant fraction of the total correlation during the highly relevant first picosecond of dynamics in many cases (some sources in the literature [10,11] indicate that the average time it takes for an excitation to trap to the reaction center is 1 ps after it arrives from the chlorosome antenna). In other cases, these quantities are equivalent and contribute a non-negligible fraction of the total correlation

during the first picosecond. This contribution indicates that nonclassical spatial correlations may be playing a role in the efficient transfer of an excitation from the chlorosome antenna to the reaction center. Our final contribution is to study the relative entropy of entanglement without its optimization restricted to the single-excitation subspace, and we find that it can be significantly less than the restricted relative entropy of entanglement while only using just a small fraction of doubly excited states in the optimization.

We structure this paper as follows. We first briefly review the dynamical model of the FMO protein complex, the definition of the quantum discord, and the definition of the relative entropy of entanglement, and we then discuss how to compute these quantities in the FMO protein complex model. Our analytic result states that the relative entropy of entanglement, when restricted to the zero- and single-excitation subspace, is equal to a simple formula that is a difference of entropies. The Appendix provides a proof of this theorem. Section IV presents the results of our numerical simulations under various initial configurations and temperatures, and Sec. V discusses the unrestricted optimization of the relative entropy of entanglement. We then conclude with observations and open questions for future research.

## II. REVIEW

### A. FMO complex dynamics

The FMO protein complex is the crucial light-harvesting component of the green sulfur bacteria *Prosthecochloris aestuarii*, which develop in dimly lit, anoxic environments such as stratified lakes or sulfur springs [37]. It is a trimer, consisting of three identical subunits. We study one unit of the trimer, consisting of seven bacteriochlorophyll sites that act as a "molecular wire," transferring energetic excitations from a photon-receiving antenna to a reaction center. A photon impinges on the antenna, producing an electronic excitation, dubbed an exciton, that then proceeds to the unit with seven sites. While traversing the seven sites, the exciton can either recombine, corresponding to an energetic loss, or trap to the reaction center for energy storage.

We characterize the quantum state of the exciton as a density operator in the site basis:

$$\rho \equiv \sum_{m,n \in \{G,1,\dots,7,S\}} \rho_{m,n} |m\rangle \langle n|,$$

where the state  $|m\rangle$  indicates that the exciton is present at site  $m$ . The sites can be any of the seven sites in the protein complex  $m \in \{1, \dots, 7\}$ , a ground state  $|G\rangle$  that represents the loss or recombination of the exciton, or a sink state  $|S\rangle$  that implies that the exciton has trapped to the reaction center. We adopt the following "qubit" convention in this work (as adopted in previous works [17,38,39]), by assigning site states to tensor-product states:

$$\begin{aligned} |G\rangle &\equiv |g\rangle_1 |g\rangle_2 |g\rangle_3 |g\rangle_4 |g\rangle_5 |g\rangle_6 |g\rangle_7 |g\rangle_S, \\ |1\rangle &\equiv |e\rangle_1 |g\rangle_2 |g\rangle_3 |g\rangle_4 |g\rangle_5 |g\rangle_6 |g\rangle_7 |g\rangle_S, \\ &\vdots \\ |7\rangle &\equiv |g\rangle_1 |g\rangle_2 |g\rangle_3 |g\rangle_4 |g\rangle_5 |g\rangle_6 |e\rangle_7 |g\rangle_S, \\ |S\rangle &\equiv |g\rangle_1 |g\rangle_2 |g\rangle_3 |g\rangle_4 |g\rangle_5 |g\rangle_6 |g\rangle_7 |e\rangle_S, \end{aligned}$$

where  $g$  indicates the absence of an excitation and  $e$  indicates the presence of an excitation at a particular site. The excitation number is a conserved quantity in the absence of light-matter interaction events [40], and this observation restricts the protein dynamics to a zero- and single-excitation subspace. Thus, the above nine states are the only states that we consider for the exciton while it traverses the seven sites.

Observe that “tracing over any site” in this qubit representation has the effect of placing the population term for that site into the population of the ground state. For example, suppose that we trace over all sites except for the first one. The resulting density matrix has the form

$$(\rho_{GG} + \rho_{22} + \cdots + \rho_{77} + \rho_{SS}) |G\rangle \langle G| + \rho_{11} |1\rangle \langle 1| + \rho_{1G} |1\rangle \langle G| + \rho_{G1} |G\rangle \langle 1|.$$

Such manipulations are important for computing correlation measures for any bipartite cut of the sites in the FMO complex.

Evolution of the density matrix occurs according to a combination of both coherent and incoherent dynamics. A tight-binding Hamiltonian of the following form governs coherent evolution across the seven site states  $|1\rangle, \dots, |7\rangle$ :

$$H \equiv \sum_m E_m |m\rangle \langle m| + \sum_{n < m} V_{nm} (|n\rangle \langle m| + |m\rangle \langle n|),$$

where  $E_m$  is the relative energy at site  $m$  and  $V_{nm}$  represents a coupling between sites  $n$  and  $m$  (see Refs. [11,15,16] for the Hamiltonian that governs evolution). The third site has the lowest energy of all seven sites and is closest to the reaction center, and it is for these reasons that researchers suggest that the objective of the molecular wire is to transmit the excitation as quickly as possible to the third site [8–11]. The off-diagonal terms lead to coherent couplings between sites—the strongest couplings are between the first and second sites, the fourth and fifth sites, and the fifth and sixth sites. Recent work determines the energy landscape of the FMO complex which reveals coherent pathways the excitation may traverse to get to the third site [24,41].

A set of three Lindblad superoperators governs incoherent evolution of the FMO complex, and each superoperator has a phenomenological justification for its presence in the evolution [8,9,11,16]. The first incoherent mechanism  $\mathcal{L}_{\text{diss}}$  is due to recombination or loss of the exciton, acting like an amplitude damping mechanism. The second incoherent mechanism  $\mathcal{L}_{\text{sink}}$  is due to trapping of the excitation from the third site to the reaction center. The final decoherence mechanism  $\mathcal{L}_{\text{deph}}$  is a local dephasing at each site, due to unavoidable interaction with the surrounding protein environment. Reference [9] shows how to relate the dephasing rate to the temperature of the system, under a particular decoherence model (we employ this relation in our numerical study in this paper). References [8,9,11,16] describe in detail the decoherence mechanisms in the FMO complex. Despite the Markovian nature of the evolution, it describes the dynamics reasonably accurately [9] (though see the recent work on non-Markovian evolution in the FMO complex [18,42]).

Putting everything together, the following master equation gives the full evolution of the density matrix  $\rho$ :

$$\dot{\rho} = -i[H, \rho] + \mathcal{L}_{\text{diss}}(\rho) + \mathcal{L}_{\text{sink}}(\rho) + \mathcal{L}_{\text{deph}}(\rho). \quad (2)$$

Note that the above evolution induces coherences only between sites in the FMO complex, so that any off-diagonal element of the density matrix of the form  $\rho_{i,G}$  or  $\rho_{i,S}$ , where  $i \in \{1, \dots, 7\}$ , vanishes. Various sources in the literature [9] and recent experimental evidence [43] suggest that the initial state of the FMO complex is a pure excitation at site 1, a pure excitation at site 6, or a mixture of these two states, because sites 1 and 6 are closest to the antenna. We incorporate each of these cases in our simulations.

The dynamical model in (2) implies that the FMO complex exhibits both classical and quantum random walk behavior, but does not exhibit exotic “quantum stochastic walk” behavior according to Table I of Ref. [44]. The classical and quantum random walk behavior then suggests that this evolution should establish both classical and quantum correlation between sites in the complex. It is these correlations that we measure in this paper.

## B. Quantum discord

We first recall various informational measures of a quantum state before briefly reviewing the motivation for the quantum discord as a measure of quantum correlations. Suppose that two parties Alice and Bob share a quantum state  $\rho^{AB}$ . The von Neumann entropy of this state is as follows:

$$H(AB)_\rho \equiv -\text{tr}\{\rho^{AB} \log_2 \rho^{AB}\},$$

where the logarithm is base 2. The entropy  $H(AB)_\rho$  measures the uncertainty about the total quantum state  $\rho^{AB}$  in units of bits, whenever the logarithm is base 2 [45]. Similarly, we can compute the marginal entropies  $H(A)$  and  $H(B)$ —these entropies are with respect to the respective reduced states  $\rho^A$  and  $\rho^B$ , obtained by a partial trace over Bob or Alice’s share of the state  $\rho^{AB}$ .

The quantum mutual information  $I(A; B)$  is a measure of the total correlations, both classical and quantum, shared between two parties, where

$$I(A; B)_\rho \equiv H(A)_\rho + H(B)_\rho - H(AB)_\rho. \quad (3)$$

The quantum mutual information admits a natural operational interpretation as the amount of noise necessary to destroy all correlations present in a bipartite state [46]. Its other operational interpretations are as the maximum amount of secret information that one party can send to another if they use a shared state as the basis for a one-time pad cryptosystem [47], the entanglement-assisted classical capacity of a quantum channel [48–50], and more recently the amount of private quantum information that a sender can transmit to a receiver while being eavesdropped on by a uniformly accelerating third party [51]. All of these operational interpretations justify the notion of the quantum mutual information measuring correlations between two parties in units of bits.

Suppose now that Alice would like to extract classical information from the quantum state  $\rho^{AB}$ . She performs a von Neumann measurement  $\{|x\rangle \langle x|\}$  on her share of the state, where the states  $\{|x\rangle\}$  form an orthonormal basis. If Alice obtains classical result  $x$  from the measurement, the resulting conditional quantum state of the whole system is

$$|x\rangle \langle x|^X \otimes \rho_x^B,$$

where

$$\rho_x^B \equiv \frac{1}{p(x)} \text{Tr}_X \{ (|x\rangle \langle x|^X \otimes I^B) \rho^{AB} (|x\rangle \langle x|^X \otimes I^B) \}, \quad (4)$$

$$p(x) \equiv \text{Tr} \{ |x\rangle \langle x|^X \rho^A \}, \quad (5)$$

and we now label Alice's system with  $X$  because it is classical. If we then take the expectation over all of Alice's outcomes, the description of the system is a classical-quantum state:

$$\sigma^{XB} \equiv \sum_x p(x) |x\rangle \langle x|^X \otimes \rho_x^B. \quad (6)$$

We might think that a natural measure of the classical correlations present in a bipartite state is the amount of correlations in the resulting classical-quantum state:

$$I_c(A; B)_\rho \equiv \max_{\{\Lambda^A\}} I(X; B)_\sigma. \quad (7)$$

The above expression features a maximization over all of the von Neumann measurements  $\Lambda^A$  that Alice could perform. These measurements result in a state of the form  $\sigma$  in (6), and the quantum mutual information  $I(X; B)_\sigma$  is with respect to such a state. In fact, Henderson and Vedral proposed such a measure [28], and Devetak and Winter later justified this measure by providing an operational interpretation of it as the maximum amount of common randomness (perfect classical correlations) that two parties can extract from a bipartite quantum state [52].

The two correlation measures in (3) and (7), the first a measure of total correlations and the second a measure of classical correlations, suggest that a measure of the quantum correlations should be the difference of these two quantities. The *quantum discord*  $D(A; B)_\rho$  is such a measure [29,53], defined as the difference of total and classical correlations:

$$D(A; B)_\rho \equiv I(A; B)_\rho - I_c(A; B)_\rho. \quad (8)$$

The discord is always non-negative, by the quantum data processing inequality of quantum information theory [54], and it is generally not symmetric with respect to the parties  $A$  and  $B$ :

$$\exists \rho: D(A; B)_\rho \neq D(B; A)_\rho.$$

It captures all of the quantum correlations, including entanglement, but also the quantumness in separable states of the form in (1). Zurek has suggested a physical interpretation of the discord as the difference in efficiency between quantum and classical Maxwell's demons [55], but it still lacks a clear operational interpretation in the sense of Refs. [46–52]. Nevertheless, we still employ the discord as a measure of the quantum correlations in the FMO complex.

We can rewrite the quantum discord as the following expression:

$$D(A; B)_\rho = I(B|A)_\rho + \min_{\{\Pi_x\}} \sum_x p(x) H(\rho_x^B), \quad (9)$$

by performing straightforward manipulations of the entropies in (8). In the above,  $I(A|B)$  is the coherent information [54], equal to the negative of a conditional entropy:

$$I(B|A)_\rho = -H(B|A)_\rho = H(A)_\rho - H(AB)_\rho,$$

and the probabilities  $p(x)$  and conditional density operators are as they appear respectively in (4) and (5).

### C. Quantum discord and the FMO protein complex

We briefly discuss an example illustrating how we compute the quantum discord for the sites in the FMO complex. Suppose that we would like to consider the quantum discord with system  $A$  consisting of site 3 and system  $B$  consisting of sites 1 and 2. We first trace out all systems other than site 1, 2, or 3, leaving a  $4 \times 4$  density matrix with support in the following basis:

$$\{|g\rangle_1 |g\rangle_2 |g\rangle_3, |e\rangle_1 |g\rangle_2 |g\rangle_3, |g\rangle_1 |e\rangle_2 |g\rangle_3, |g\rangle_1 |g\rangle_2 |e\rangle_3\}.$$

A measurement of the  $A$  system consisting of rank-1 projective operators in this case takes a particularly simple form because the  $A$  system is a qubit system. That is, such a measurement is of the form  $\{|\varphi\rangle\langle\varphi|, |\varphi^\perp\rangle\langle\varphi^\perp|\}$  where  $|\varphi\rangle \equiv \cos(\theta) |g\rangle + e^{i\phi} \sin(\theta) |e\rangle$ . Thus, it is straightforward to perform the optimization needed for the quantum discord in such a case. The computation of the quantum discord with more sites in the measured system simply involves a parametrization and optimization over potential rank-1 projective measurements.

### D. Relative entropy of entanglement

The relative entropy of entanglement is an entanglement measure from quantum information theory [36], and we briefly review its definition. The relative entropy  $D(\rho^{AB} || \omega^{AB})$  of two bipartite states  $\rho^{AB}$  and  $\omega^{AB}$  is as follows [54]:

$$D(\rho^{AB} || \omega^{AB}) \equiv \text{Tr} \{ \rho^{AB} \log_2 \rho^{AB} \} - \text{Tr} \{ \rho^{AB} \log_2 \omega^{AB} \}. \quad (10)$$

This measure, in some sense, quantifies the “distance” between two bipartite states, but it is not a distance measure in the strict mathematical sense because it fails to be symmetric, although this intuition is useful for constructing an entanglement measure. We might naturally expect a good measure of entanglement to be the distance of a given bipartite state to the closest separable state  $\sigma^{AB} \equiv \sum_i p(i) \sigma_i^A \otimes \sigma_i^B$ . The relative entropy of entanglement  $R(\rho^{AB})$  is such a measure, defined as the minimization of the relative entropy over all separable states:

$$R(\rho^{AB}) \equiv \min_{\sigma \in \mathcal{S}} D(\rho^{AB} || \sigma^{AB}),$$

where  $\mathcal{S}$  is the class of separable states. This measure satisfies the properties of an entanglement measure and appears extensively in the quantum information theory literature [36]. We mention that the authors of Ref. [17] employed a variation of this entanglement measure for determining quantum correlations in the FMO complex, but they considered the global relative entropy of entanglement rather than a bipartite version of it as we consider in this work. The variation that they employed was to restrict the minimization to the single-excitation subspace, but the resulting measure is not an entanglement monotone in the strict sense [18]. In this paper, we calculate both the single-excitation relative entropy of entanglement and the unrestricted relative entropy of entanglement for comparative purposes.



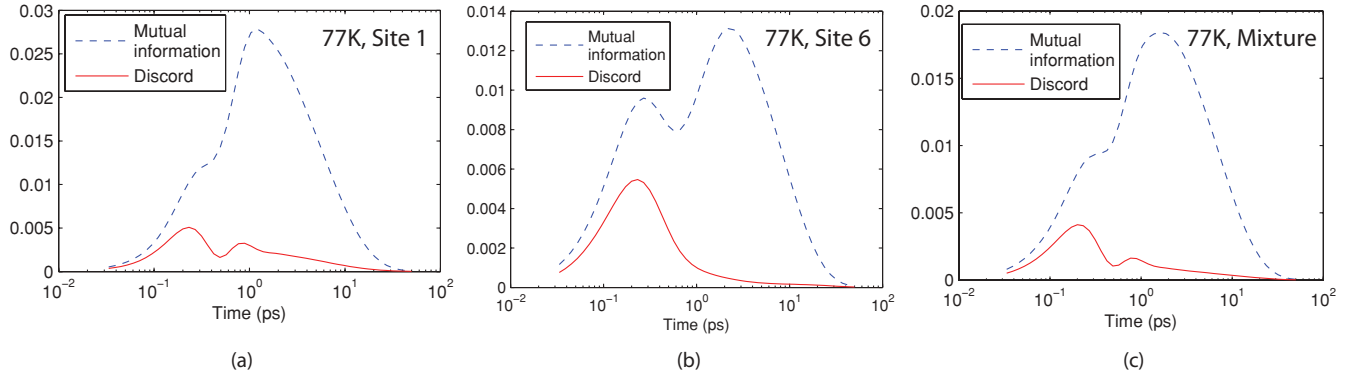


FIG. 1. (Color online) Mutual information  $I(A; B)$  and quantum discord  $D(A; B)$  with system  $A$  as site 3 and system  $B$  as sites 1 and 6. The figure plots these quantities at cryogenic temperature (77 K) as a function of time when the initial state is (a) a pure state at the first site, (b) a pure state at the sixth state, and (c) an equal mixture of the two previous states. In each of the above plots, the quantum discord is a significant fraction of the total correlations during the first picosecond.

### III. FORMULA FOR THE SINGLE-EXCITATION RELATIVE ENTROPY OF ENTANGLEMENT

The restriction of dynamics to the zero- and single-excitation subspace allows for significant simplifications to the theory of energetic transfer in the FMO complex. We can also apply this restriction to the relative entropy of entanglement, by restricting the optimization over separable states to the zero- and single-excitation subspace. Let  $R_e(\rho^{AB})$  denote the relative entropy of entanglement with this restriction applied to its optimization. Theorem 1 below states that  $R_e(\rho^{AB})$  is equal to a simple formula that is a difference of entropies. Thus, the theorem significantly simplifies the computation of this quantity.

*Theorem 1.* Consider a density operator  $\rho^{AB}$  restricted to the zero- and single-excitation subspace. Let

$$\overline{\Delta}(\rho^{AB}) \equiv \alpha |G\rangle\langle G| + \rho_e^A \otimes |G\rangle\langle G|^B + |G\rangle\langle G|^A \otimes \rho_e^B,$$

where  $\alpha$  is the population of the ground state,  $\rho_e^A$  is the projection of Alice's part of  $\rho^{AB}$  into the single-excitation subspace, and  $\rho_e^B$  is defined in a similar way. Suppose that the dynamics for this density operator never induces any

coherences between the zero- and single-excitation subspaces [as in the dynamics in (2)]. Then the single-excitation relative entropy of entanglement  $R_e(\rho)$  is equal to the difference between the entropies of  $\overline{\Delta}(\rho^{AB})$  and  $\rho^{AB}$ :

$$R_e(\rho^{AB}) = H(\overline{\Delta}(\rho^{AB})) - H(\rho^{AB}).$$

The full proof appears in the Appendix. It exploits standard properties of the von Neumann entropy and a perturbative argument.

### IV. SIMULATION RESULTS

We conducted several simulations at both cryogenic temperature (77 K) and physiological temperature (300 K) and for the initial state being a pure state at sites 1, 6, and a mixture of the previous two. These simulations calculate the quantum mutual information, quantum discord, and single-excitation relative entropy of entanglement with respect to several ‘‘bipartite cuts’’ of the sites in the FMO complex. Throughout this section, we refer to quantum discord, but all our simulations indicated that the single-excitation relative entropy of entanglement is equal to the quantum discord. These results provide strong evidence that the quantum discord is

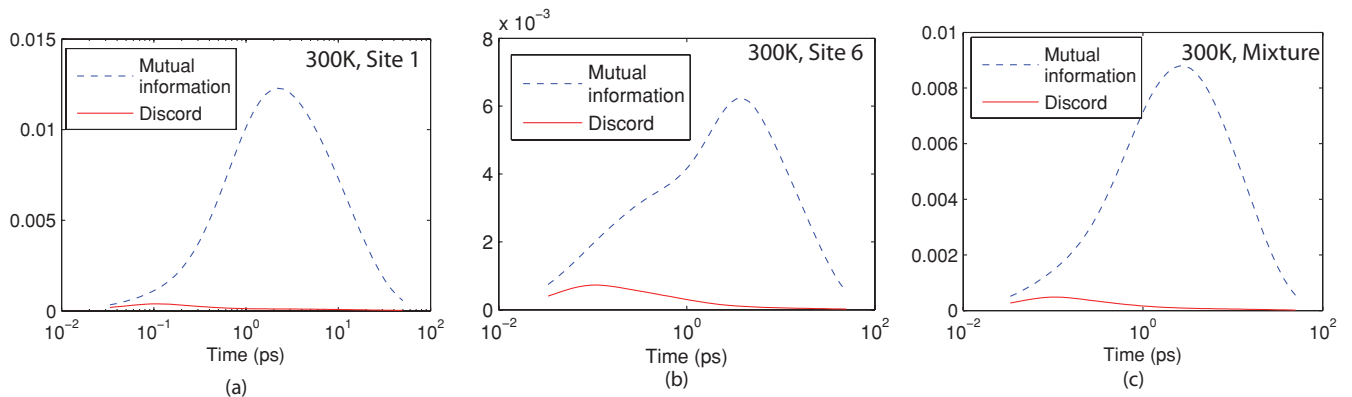


FIG. 2. (Color online) Mutual information  $I(A; B)$  and quantum discord  $D(A; B)$  with system  $A$  as site 3 and system  $B$  as sites 1 and 6. The figure plots these quantities at physiological temperature (300 K) as a function of time when the initial state is (a) a pure state at the first site, (b) a pure state at the sixth state, and (c) an equal mixture of the two previous states. In each of the above figures, the quantum discord is a non-negligible fraction of the total correlation during the first picosecond.

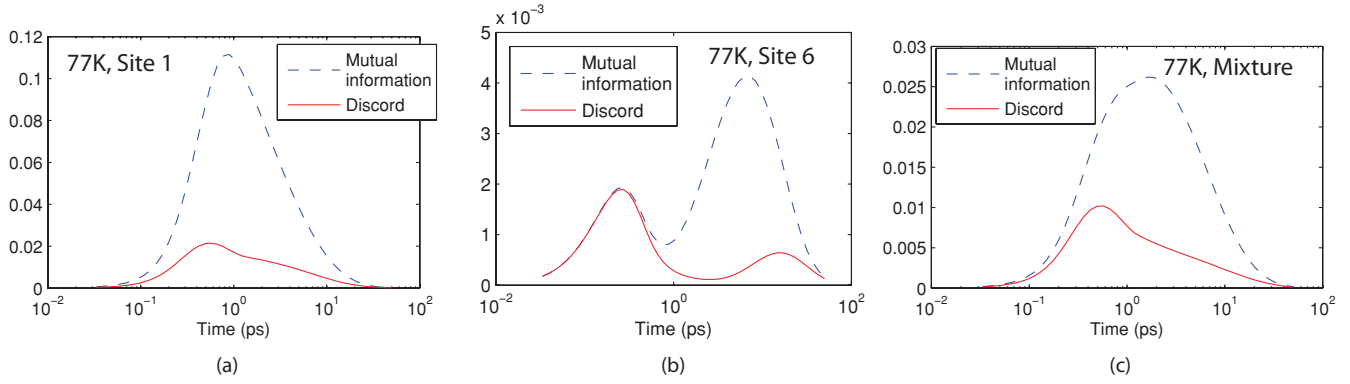


FIG. 3. (Color online) Mutual information  $I(A; B)$  and quantum discord  $D(A; B)$  with system  $A$  as site 3 and system  $B$  as sites 1 and 2. The figure plots these quantities at cryogenic temperature (77 K) as a function of time when the initial state is (a) a pure state at the first site, (b) a pure state at the sixth state, and (c) an equal mixture of the two previous states. In each of the above cases, the quantum discord is a significant fraction of the total correlation during the first picosecond. In fact, for the second case, the quantum discord contributes nearly all of the total correlation during the first picosecond.

equal to the formula in Theorem 1 for these cases, but a general proof of this conjecture eludes us for now. Our different simulation cases are as follows:

(1) We first considered the cut where system  $A$  consists of site 3 and system  $B$  consists of sites 1 and 6. We picked this cut because the initial state of the complex is at site 1, 6, or the mixture, and the objective of the FMO “molecular wire” is to transfer the excitation from these initial sites to site 3. If spatial quantum correlations play a role in the transfer of the excitation, one would expect a state with this bipartite cut to register a non-negligible amount of quantum discord.

(2) The next bipartite cut that we considered is with the  $A$  system consisting of sites 1 and 2 and the  $B$  system consisting of site 3. We picked such a cut because recent analysis of the FMO Hamiltonian [41] suggests that a superposition state of sites 1 and 2 gives an efficient energetic pathway for the excitation to transfer to site 3. The energy of the superposed state is closer to the energy of site 3 than it is to the energy of either site 1 or site 2. We would again expect that such a cut would register a non-negligible amount of quantum

discord if quantum correlations play a role in the transfer of the excitation.

(3) Finally, after conducting the above simulations, we conducted simulations with respect to the cut where system  $A$  consists of site 3 and system  $B$  consists of all other sites. The quantum mutual information for this case should be larger than for the case of the other cuts, by the quantum data processing inequality.

Figure 1 plots the results of the first simulation for cryogenic temperature and for each initial state. The figure indicates that the quantum discord contributes a significant fraction of the total correlation for short time scales (less than 1 ps). This contribution of the quantum discord to total correlation is significant, considering that the average transfer time of the excitation to site 3 occurs around the order of 1 ps in our model. For longer time scales (greater than 1 ps), the total correlation between  $A$  (sites 1 and 6) and  $B$  (site 3) increases to its maximum at around 2–4 ps, and the quantum discord no longer contributes any significant amount to the total correlation. Even though the total correlation rises so

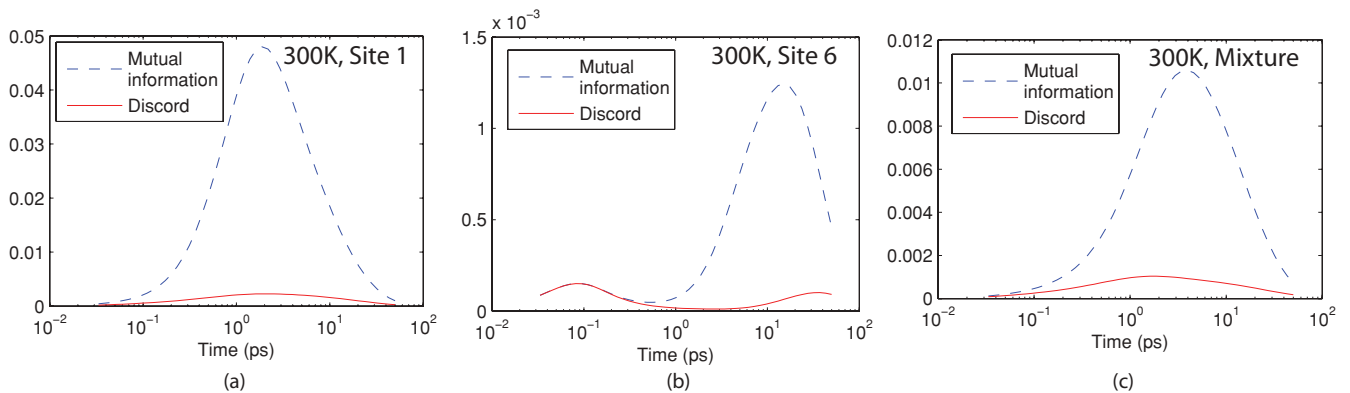


FIG. 4. (Color online) Mutual information  $I(A; B)$  and quantum discord  $D(A; B)$  with system  $A$  as site 3 and system  $B$  as sites 1 and 2. The figure plots these quantities at physiological temperature (300 K) as a function of time when the initial state is (a) a pure state at the first site, (b) a pure state at the sixth state, and (c) an equal mixture of the two previous states. In each of the above cases, the quantum discord contributes a fraction of the total correlation during the first picosecond. In the second case, it again contributes nearly all of the total correlation during the first picosecond.

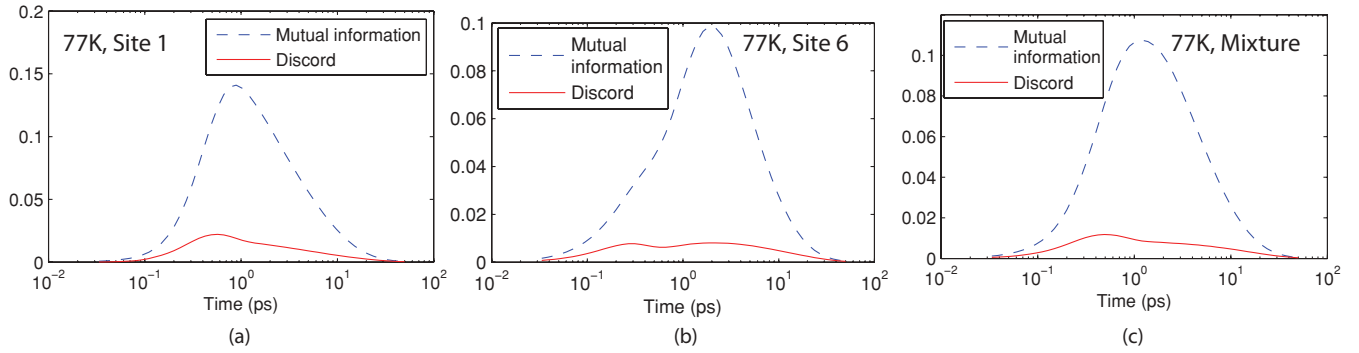


FIG. 5. (Color online) Mutual information  $I(A; B)$  and quantum discord  $D(A; B)$  with system  $A$  as site 3 and system  $B$  as all other sites (1,2,4–7). The figure plots these quantities at cryogenic temperature (77 K) as a function of time when the initial state is (a) a pure state at the first site, (b) a pure state at the sixth state, and (c) an equal mixture of the two previous states. The quantum discord contributes a significant fraction of the total correlation during the first picosecond.

much higher for longer time scales than it does for shorter time scales, the increase and peak are not relevant for excitation transfer, i.e., “they arrive too late,” given that this transfer occurs on the order of 1 ps. The total correlation then washes away as time increases beyond 10 ps, and it should nearly vanish for times around 1 ns because this time is the average recombination time of the exciton, and no correlations should persist after a recombination.

Figure 2 plots the results of the first simulation for physiological temperature. The difference between cryogenic and physiological temperature is a qualitative shrinking by a factor of 2, but the fraction of quantum discord that contributes to the total correlation for short time scales is lower than it is for cryogenic temperatures. The local dephasing at each site acts to destroy both total and quantum correlation, but it appears to have a more harmful effect on quantum correlation. Despite the low amount of quantum discord registered at physiological temperature, it could still be that a light-harvesting complex is harnessing this small amount of quantumness (which is a significant fraction of the total correlation) on this short time scale to enhance excitation transfer.

Figures 3 and 4 plot the results of the second simulation for both respective temperatures and for each initial state. These results are qualitatively similar to those for the previous bipartite cut, but the most striking difference is that the

quantum discord contributes all of the correlation (it is equal to the quantum mutual information) for short time scales when the initial state is at site 6 for both cryogenic and physiological temperatures [see Figs. 3(b) and 4(b)].

Figures 5 and 6 plot the results of our final simulation, where the bipartite cut has system  $B$  as site 3 and system  $A$  as all other sites. The results for quantum discord are again qualitatively similar to the previous results, but the quantum mutual information is significantly higher than for the previous cases (this is expected because the quantum data processing inequality states that correlations can only decrease when subsystems are discarded). The quantum discord again contributes a significant fraction of the total correlation for short time scales and contributes only a small fraction for later time scales. Again, physiological temperature decoherence mitigates the presence of quantumness.

## V. COMPARISON OF THE QUANTUM DISCORD WITH THE STANDARD RELATIVE ENTROPY OF ENTANGLEMENT

In this section, we focus on computing the relative entropy of entanglement in (10) without the assumption that the set of separable states  $\sigma^{AB}$  involved in the minimization of  $D(\rho^{AB} || \sigma^{AB})$  is limited to the single-excitation subspace. This

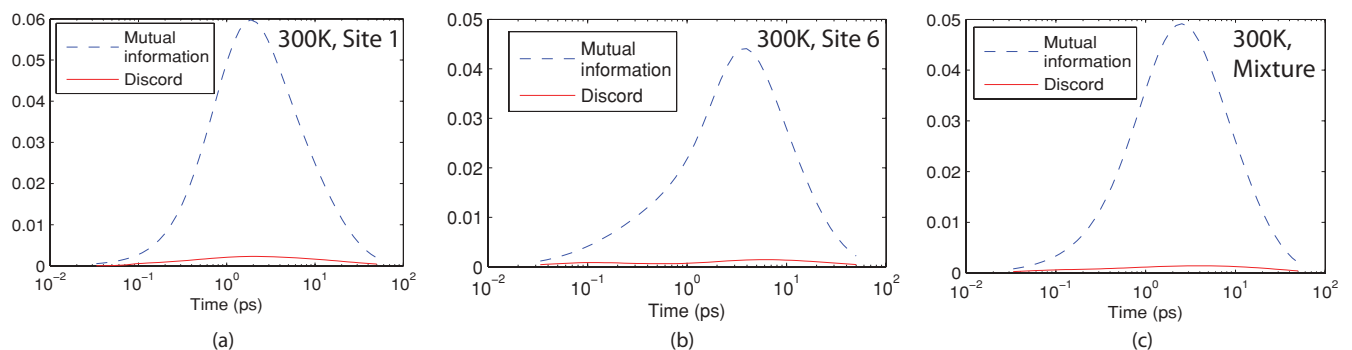


FIG. 6. (Color online) Mutual information  $I(A; B)$  and quantum discord  $D(A; B)$  with system  $A$  as site 3 and system  $B$  as all other sites (1,2,4–7). The figure plots these quantities at physiological temperature (300 K) as a function of time when the initial state is (a) a pure state at the first site, (b) a pure state at the sixth state, and (c) an equal mixture of the two previous states. The quantum discord does not contribute a large fraction of the total correlation here.

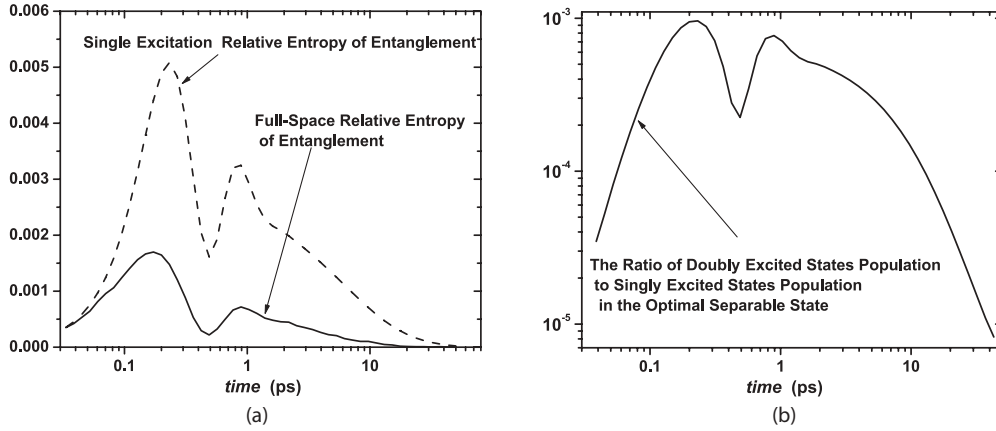


FIG. 7. (a) This figure plots the results of simulations of the FMO complex at 77 K and calculates both the single-excitation relative entropy of entanglement and the full relative entropy of entanglement for  $A = 1,6$  and  $B = 3$ . (b) The ratio of the number of doubly excited states to the number of singly excited states in the optimal separable state for the relative entropy of entanglement is rather small.

implies that  $\sigma^{AB}$  may include multiply excited states (for example, states for which both systems  $A$  and  $B$  carry an exciton).

A question may arise as to why such multiply excited states are relevant for the optimization of the relative entropy of entanglement. After all, the Hamiltonian of the system commutes with the operator corresponding to the total number of excitations in the system, and the dissipation operators in (2) only decrease the number of excitations by dumping them to the sink or to the reaction center. There are two different ways to answer this question. The first one is simple yet somewhat formal—Vedral [36] established the relative entropy of entanglement in the context of quantum information theory as a measure of entanglement for a general set of states with no subspace limitations imposed. Therefore, even though the form of the specific Hamiltonian and dissipation terms in (2) leads to the absence of multiply excited states in the density operator, there is no particular reason to consider that multiply excited states and the mode of preparation of a state are irrelevant in this setting. From this perspective, entanglement is determined solely by the state rather than by the history and mode of state evolution. The relative entropy of entanglement is a measure of the “distance” of a state from the closest separable state, and excluding multiply excited states from the set of separable states introduces a distortion to the original concept. Actually, the measure of such a distortion may be rather large, as we found out by performing optimization of  $D(\rho^{AB}||\sigma^{AB})$  in the full space [see Fig. 7(a)].

Our second answer is more physically motivated. In general, while analyzing the exciton dynamics in a light-harvesting system, one assumes that the intensity of light, which determines the photon flux, is quite small. Then it follows that the probability of simultaneous creation of two excitations is negligible. By performing the optimization of  $D(\rho^{AB}||\sigma^{AB})$  in the full space, which includes multiply excited states that can have the form  $|E\rangle^A|E\rangle^B$ , and computing the amount of multiply excited state population in the closest separable state  $\sigma^{AB}$ , we can set up a limit for the light intensity when the single-excitation assumption will become meaningless even in the context of excitation-preserving dynamics. In

accordance with Caratheodory’s theorem, we generated the generic separable state  $\sigma^{AB}$  as a sum of  $2^6 = 64$  arbitrary pure separable states  $\sum_{n=1}^{64} c_n |\psi_n\rangle\langle\psi_n|$ . Here, we limited our computation to a simple example where site  $A = 1,6$  and site  $B = 3$ , such that

$$|\psi_n\rangle = (\alpha_0|g\rangle_1|g\rangle_6 + \alpha_1|e\rangle_1|g\rangle_6 + \alpha_2|g\rangle_1|e\rangle_6 + \alpha_3|e\rangle_1|e\rangle_6) \otimes (\beta_1|g\rangle_3 + \beta_2|e\rangle_3).$$

The optimization is performed by the gradient method in the space of coefficients  $c_n$ ,  $\alpha_i$ , and  $\beta_j$ . Figure 7(a) shows results of the computation for  $T = 77$  K. We note that relative entropy of entanglement for the single-excitation-subspace case has a similar shape to the full-space relative entropy of entanglement, but it is approximately five times smaller. Figure 7(b) demonstrates that the population of doubly excited states in the optimal separable state is negligibly small—it is three to five orders of magnitude smaller than the population of singly excited states. We find it remarkable that such a negligible admixture of doubly excited states changes the relative entropy of entanglement by more than a factor of 5.

## VI. CONCLUSIONS

We presented results quantifying the quantum correlations present in a biological system at cryogenic and physiological temperatures. Theorem 1 proves that the single-excitation relative entropy of entanglement admits a simple form. We then simulated the dynamics of the FMO complex and calculated the quantum discord and the quantum mutual information for various phenomenologically motivated bipartite cuts of the sites in the FMO protein complex. It is surprising that the quantum discord and the single-excitation relative entropy of entanglement are equivalent for these simulations, but we have not been able to find a general proof that the quantum discord of this system is equivalent to the formula in Theorem 1. The results of our simulations indicate that quantum correlations contribute a significant fraction of the total correlation during the first picosecond of dynamics in many cases. Our last contribution was to study the relative entropy of entanglement with an unrestricted optimization, and we found that a small



fraction of doubly excited states contribute significantly to reducing the relative entropy of entanglement.

Open questions remain for this line of research. Our last contribution above suggests an intriguing open question of whether optimizing the relative entropy of entanglement over a single-excitation subspace, as done here and in Ref. [17], is operationally justified. We should also compute the correlation of the quantum discord with the measure of transfer time in Ref. [9] of the excitation from the antenna to the reaction center. This correlation might indicate how relevant quantumness is for the transfer of the excitation. Finally, it might be interesting to determine how efficiency or transfer time is affected by differing amounts of quantum discord, if there can be efficient energy transfer without quantum discord, and how discord compares with entanglement in the general case.

### ACKNOWLEDGMENTS

The authors acknowledge useful discussions with Mohan Sarovar and thank the anonymous referees for useful comments. K.B. acknowledges support from the Office of Naval Research under Grant No. N000140811249. M.M.W. acknowledges support from the MDEIE (Québec) PSR-SIIRI international collaboration grant. D.B.U. acknowledges support from the National Science Foundation under Grants No. PHY-0545390 and PHY-1005709.

### APPENDIX

We first establish some notation before proving Theorem 1. Let our zero- and single-excitation space be spanned by the following states:

$$\begin{aligned} |G\rangle^{AB} &\equiv |g\rangle_1 |g\rangle_2 \cdots |g\rangle_n, \\ |1\rangle^{AB} &\equiv |e\rangle_1 |g\rangle_2 \cdots |g\rangle_n, \\ &\vdots \\ |n\rangle^{AB} &\equiv |g\rangle_1 |g\rangle_2 \cdots |e\rangle_n. \end{aligned}$$

The number of states is thus  $n + 1$ . We introduce a bipartite splitting of the above states so that the corresponding subsystems  $A$  and  $B$  are spanned by  $\{|G\rangle^A, |1\rangle^A, \dots, |n_a\rangle^A\}$  and  $\{|G\rangle^B, |1\rangle^B, \dots, |n_b\rangle^B\}$ , respectively, using the same convention as above. Note that  $n_a + n_b + 1 = n$ , and the original basis written in terms of the split bases reads

$$\{|G\rangle^A |G\rangle^B, |k\rangle^A |G\rangle^B, |G\rangle^A |j\rangle^B\},$$

where  $k = 1, \dots, n_a$  and  $j = 1, \dots, n_b$ . Let  $\Pi_e^A$  and  $\Pi_e^B$  denote the projectors onto the excited subspaces of the individual subsystems of  $A$  and  $B$ :

$$\Pi_e^A \equiv \sum_{k=1}^{n_a} |k\rangle\langle k|^A, \quad \Pi_e^B \equiv \sum_{j=1}^{n_b} |j\rangle\langle j|^B. \quad (\text{A1})$$

The projector onto the full bipartite single-excitation subspace is as follows:

$$\Pi_e^{AB} \equiv |G\rangle\langle G|^A \otimes \Pi_e^B + \Pi_e^A \otimes |G\rangle\langle G|^B. \quad (\text{A2})$$

Let  $\Pi_g^{AB} \equiv |G\rangle\langle G|^A \otimes |G\rangle\langle G|^B$ . Then  $\Pi_g^{AB} + \Pi_e^{AB}$  is a projector onto the zero- and single-excitation subspace. We have that

$\langle G|^{AB} \rho^{AB} |k\rangle^{AB} = 0$  because the dynamics in (2) does not induce any correlations between the ground state and the single-excitation subspace of the density matrix  $\rho^{AB}$ . The following chain of inequalities then gives another way to write the density matrix  $\rho^{AB}$  that is more useful to us:

$$\begin{aligned} \rho^{AB} &= (\Pi_g^{AB} + \Pi_e^{AB}) \rho^{AB} (\Pi_g^{AB} + \Pi_e^{AB}) \\ &= \alpha \Pi_g^{AB} + \Pi_e^{AB} \rho^{AB} \Pi_g^{AB} \\ &\quad + \Pi_g^{AB} \rho^{AB} \Pi_e^{AB} + \Pi_e^{AB} \rho^{AB} \Pi_e^{AB} \\ &= \alpha \Pi_g^{AB} + \Pi_e^{AB} \rho^{AB} \Pi_e^{AB} \\ &= \alpha \Pi_g^{AB} + (|G\rangle\langle G|^A \otimes \Pi_e^B + \Pi_e^A \otimes |G\rangle\langle G|^B) \\ &\quad \times \rho^{AB} (|G\rangle\langle G|^A \otimes \Pi_e^B + \Pi_e^A \otimes |G\rangle\langle G|^B) \\ &= \alpha \Pi_g + (|G\rangle\langle G|^A \otimes \Pi_e^B) \rho^{AB} (|G\rangle\langle G|^A \otimes \Pi_e^B) \\ &\quad + (|G\rangle\langle G|^A \otimes \Pi_e^B) \rho^{AB} (\Pi_e^A \otimes |G\rangle\langle G|^B) \\ &\quad + (\Pi_e^A \otimes |G\rangle\langle G|^B) \rho^{AB} (|G\rangle\langle G|^A \otimes \Pi_e^B) \\ &\quad + (\Pi_e^A \otimes |G\rangle\langle G|^B) \rho^{AB} (\Pi_e^A \otimes |G\rangle\langle G|^B) \\ &= \alpha \Pi_g + \rho_e^A \otimes |G\rangle\langle G|^B + |G\rangle\langle G|^A \otimes \rho_e^B + \tau^{AB}. \end{aligned} \quad (\text{A3})$$

The first equality follows because  $\rho^{AB}$  exists in the zero- and single-excitation subspace. The second equality follows by expanding. The third equality follows because the density operator  $\rho^{AB}$  does not have any correlations between the ground state  $|G\rangle$  and any excited state. The fourth equality follows from the relation in (A2). The fifth equality follows by expanding, and the last follows from the definitions

$$\rho_e^A \equiv \text{Tr}_B \{ (\Pi_e^A \otimes |G\rangle\langle G|^B) \rho^{AB} (\Pi_e^A \otimes |G\rangle\langle G|^B) \}, \quad (\text{A4})$$

$$\rho_e^B \equiv \text{Tr}_A \{ (|G\rangle\langle G|^A \otimes \Pi_e^B) \rho^{AB} (|G\rangle\langle G|^A \otimes \Pi_e^B) \}, \quad (\text{A5})$$

$$\begin{aligned} \tau^{AB} &\equiv (\Pi_e^A \otimes |G\rangle\langle G|^B) \rho^{AB} (|G\rangle\langle G|^A \otimes \Pi_e^B) \\ &\quad + (|G\rangle\langle G|^A \otimes \Pi_e^B) \rho^{AB} (\Pi_e^A \otimes |G\rangle\langle G|^B). \end{aligned} \quad (\text{A6})$$

The matrix  $\rho_e^A$  is the projection of  $\rho^{AB}$  into Alice's single-excitation subspace,  $\rho_e^B$  is similarly defined, and  $\tau^{AB}$  is the block-off-diagonal part of the terms existing in the single-excitation subspace.

### 1. Proof that $R_e(\rho^{AB}) = H(\overline{\Delta}(\rho^{AB})) - H(\rho^{AB})$

*Proof.* Our first candidate to maximize the relative entropy of entanglement is a state of the following form:

$$\sigma_0 = \beta \Pi_g + \sigma_e^A \otimes |G\rangle\langle G|^B + |G\rangle\langle G|^A \otimes \sigma_e^B, \quad (\text{A7})$$

because it is in the most general form of a single-excitation separable state with no correlation between the ground state and the other states. The operators  $\sigma_e^A$  and  $\sigma_e^B$  are some positive operators that exist in the single-excitation subspaces with respective projectors  $\Pi_e^A$  and  $\Pi_e^B$ . So, for now, we restrict the minimization of the relative entropy of entanglement to states of the above form, leading to the following minimization:

$$\tilde{R}_e(\rho^{AB}) \equiv \min_{\sigma_0} \text{Tr} \{ \rho^{AB} \log_2 \rho^{AB} \} - \text{Tr} \{ \rho^{AB} \log_2 \sigma_0 \}. \quad (\text{A8})$$

We first determine a spectral decomposition of  $\sigma_e^A$  and  $\sigma_e^B$  as follows:

$$\sigma_e^A = \sum_{k=1}^{n_a} a_k |\phi_k\rangle \langle \phi_k|^A, \quad \sigma_e^B = \sum_{k=1}^{n_b} b_k |\phi_k\rangle \langle \phi_k|^B. \quad (\text{A9})$$

Let  $\omega^A \equiv \log_2(\sigma_e^A)$  and  $\omega^B \equiv \log_2(\sigma_e^B)$ . The following equalities then hold

$$\begin{aligned} \tau^{AB} \log_2 \sigma_0 &= [(\Pi_e^A \otimes |G\rangle \langle G|^B) \rho^{AB} (|G\rangle \langle G|^A \otimes \Pi_e^B) \\ &\quad + (|G\rangle \langle G|^A \otimes \Pi_e^B) \rho^{AB} (\Pi_e^A \otimes |G\rangle \langle G|^B)] \\ &\quad \times \log_2 (\alpha \Pi_g + \sigma_e^A \otimes |G\rangle \langle G|^B \\ &\quad + |G\rangle \langle G|^A \otimes \sigma_e^B) \\ &= (\Pi_e^A \otimes |G\rangle \langle G|^B) \rho^{AB} (|G\rangle \langle G|^A \otimes \omega^B) \\ &\quad + (|G\rangle \langle G|^A \otimes \Pi_e^B) \rho^{AB} (\omega^A \otimes |G\rangle \langle G|^B). \end{aligned}$$

The first equality follows by definition, and the second follows by considering the overlapping support of the different subspaces. We then find that

$$\begin{aligned} \text{Tr}\{\tau^{AB} \log_2 \sigma_0\} &= \text{Tr}\{(\Pi_e^A \otimes |G\rangle \langle G|^B) \rho^{AB} (|G\rangle \langle G|^A \otimes \omega^B) \\ &\quad + (|G\rangle \langle G|^A \otimes \Pi_e^B) \rho^{AB} (\omega^A \otimes |G\rangle \langle G|^B)\} \\ &= \text{Tr}\{(|G\rangle \langle G|^A \otimes \omega^B) (\Pi_e^A \otimes |G\rangle \langle G|^B) \\ &\quad \times \rho^{AB}\} + \text{Tr}\{(\omega^A \otimes |G\rangle \langle G|^B) \\ &\quad \times (|G\rangle \langle G|^A \otimes \Pi_e^B) \rho^{AB}\} \\ &= 0. \end{aligned}$$

The second equality follows from cyclicity of the trace, and the last equality follows because the zero- and single-excitation subspaces are orthogonal. Therefore,

$$\text{Tr}\{\rho^{AB} \log_2 \sigma_0\} = \text{Tr}\{(\rho^{AB} - \tau^{AB}) \log_2 \sigma_0\}. \quad (\text{A10})$$

Observe that  $\rho^{AB} - \tau^{AB}$  is a state of the form  $\sigma_0$  with  $\beta = \alpha$ ,  $\sigma_e^A = \rho_e^A$ , and  $\sigma_e^B = \rho_e^B$ . Consider that

$$\begin{aligned} &\text{Tr}\{(\rho^{AB} - \tau^{AB}) \log_2(\rho^{AB} - \tau^{AB})\} \\ &\geq \text{Tr}\{(\rho^{AB} - \tau^{AB}) \log_2 \sigma_0\}, \end{aligned}$$

because the relative entropy  $D((\rho^{AB} - \tau^{AB}) || \sigma_0) \geq 0$  [54]. We conclude that  $\tilde{R}_e(\rho^{AB})$  in (A8) attains its global minimum at  $\rho - \tau^{AB}$ . Thus,

$$\tilde{R}_e(\rho^{AB}) = H(\bar{\Delta}(\rho^{AB})) - H(\rho^{AB}).$$

The expression in (A7) is not the most general single-excitation separable state because it does not include coherence elements between the ground state and the single-excitation subspace. That is, matrix elements of the following form could be nonzero:

$$|G\rangle^A |G\rangle^B \langle \phi_k|^A \langle G|^B + \text{H.c.}, \quad (\text{A11})$$

$$|G\rangle^A |G\rangle^B \langle G|^A \langle \phi_k|^B + \text{H.c.} \quad (\text{A12})$$

We now show that it is not necessary to consider states of this more general form by appealing to a perturbation theory

argument [56]. Consider a solution  $\omega \equiv \rho - \tau^{AB}$  of (A8). Let us take a small shift of this solution:

$$\omega \rightarrow \omega + \epsilon (|G\rangle^A |G\rangle^B \langle \phi_k|^A \langle G|^B + \text{H.c.}). \quad (\text{A13})$$

Consider that

$$\omega |\phi_k\rangle^A |G\rangle^B = a_k |\phi_k\rangle^A |G\rangle^B \quad (\text{A14})$$

and

$$\omega |G\rangle^A |G\rangle^B = \alpha |\phi_k\rangle^A |G\rangle^B. \quad (\text{A15})$$

Since  $\omega$  is Hermitian, we can apply perturbation theory to compute the new states and energies. Brillouin-Wigner perturbation theory states that if a Schrödinger-like equation such as the one above is perturbed via

$$\omega \rightarrow \omega + \epsilon d\omega, \quad (\text{A16})$$

where  $d\omega = |G\rangle^A |G\rangle^B \langle \phi_k|^A \langle G|^B + \text{H.c.}$ , then the new states are given by

$$\begin{aligned} |\phi_k\rangle^A |G\rangle^B &\rightarrow |\phi_k\rangle^A |G\rangle^B + \epsilon \sum_{|\phi_m\rangle \neq |\phi_k\rangle^A |G\rangle^B} \frac{1}{a_k - E_m} \langle \phi_m | d\omega | \phi_k \rangle^A |G\rangle^B \\ &\quad + O(\epsilon^2). \end{aligned}$$

Here  $E_m$  refers to the eigenvalue of the state  $|\phi_m\rangle$ . Substituting for  $d\omega$ , we obtain

$$|\phi_k\rangle^A |G\rangle^B \rightarrow |\phi_k\rangle^A |G\rangle^B + \frac{\epsilon}{a_k - \alpha} |G\rangle^A |G\rangle^B + O(\epsilon^2).$$

Similarly, applying Brillouin-Wigner perturbation theory (BWPT) to the second Schrödinger-like equation above yields

$$\begin{aligned} |G\rangle^A |G\rangle^B &\rightarrow |G\rangle^A |G\rangle^B + \epsilon \sum_{|\phi_m\rangle \neq |G\rangle^A |G\rangle^B} \frac{1}{\alpha - E_m} \langle \phi_m | d\omega | G \rangle^A |G\rangle^B \\ &\quad + O(\epsilon^2). \end{aligned}$$

Again, substituting for  $d\omega$  gives

$$|G\rangle^A |G\rangle^B \rightarrow |G\rangle^A |G\rangle^B + \frac{\epsilon}{\alpha - a_k} |\phi_k\rangle^A |G\rangle^B + O(\epsilon^2).$$

Within BWPT, the eigenvalues are calculated as

$$\begin{aligned} a_k &\rightarrow a_k + \epsilon \langle \phi_k |^A \langle G |^B d\omega | \phi_k \rangle^A |G\rangle^B \\ &\quad + \sum_{|\phi_m\rangle \neq |k\rangle^A |G\rangle^B} \frac{\epsilon^2}{a_k - E_m} |\langle \phi_m | d\omega | \phi_k \rangle^A |G\rangle^B|^2 \end{aligned}$$

and similarly

$$\alpha \rightarrow \alpha + \epsilon \langle G^A | G^B d\omega | G^A \rangle | G^B \rangle + \sum_{|\phi_m\rangle \neq |G^A\rangle | G^B\rangle} \frac{\epsilon^2}{\alpha - E_m} |\langle \phi_m | d\omega | G^A \rangle | G^B \rangle|^2.$$

Using the above, we find that the eigenvectors transform up to first order as follows:

$$|\phi_k\rangle^A | G^B \rangle \rightarrow |\phi_k\rangle^A | G^B \rangle + \epsilon \frac{|G^A\rangle^A | G^B \rangle}{\alpha_k - \alpha} + O(\epsilon^2), \quad (\text{A17})$$

$$|G^A\rangle^A | G^B \rangle \rightarrow |G^A\rangle^A | G^B \rangle + \epsilon \frac{|\phi_k\rangle^A | G^B \rangle}{\alpha - a_k} + O(\epsilon^2). \quad (\text{A18})$$

Correspondingly, the eigenvalues change up to second order as follows:

$$a_k \rightarrow a_k + O(\epsilon^2), \quad (\text{A19})$$

$$\alpha \rightarrow \alpha + O(\epsilon^2), \quad (\text{A20})$$

and so

$$\omega \rightarrow \omega + \frac{\epsilon}{\alpha - a_k} \log_2 \left( \frac{\alpha}{a_k} \right) \times [ |G^A\rangle^A | G^B \rangle \langle \phi_k |^A \langle G^B | + \text{H.c.} ] + O(\epsilon^2).$$

Using

$$\text{Tr}[\rho (|G^A\rangle^A | G^B \rangle \langle \phi_k |^A \langle G^B | + \text{H.c.})] = 0 \quad (\text{A21})$$

we conclude that  $\omega = \rho - \tau^{AB}$  is the state where the relative entropy attains its global minimum.

- 
- [1] M. Arndt, T. Juffmann, and V. Vedral, *HFSP J.* **1**, 118 (2009).  
[2] S. Lloyd, *Nature Phys.* **5**, 164 (2009).  
[3] D. Abbott, J. Gea-Banacloche, P. C. W. Davies, S. Hameroff, A. Zeilinger, J. Eisert, H. Wiseman, and S. M. Bezrukov, *Fluct. Noise Lett.* **8**, C5 (2008).  
[4] *Quantum Aspects of Life*, edited by D. Abbott, P. C. W. Davies, and A. K. Pati (Imperial College Press, London, 2008).  
[5] Y.-C. Cheng and G. R. Fleming, *Annu. Rev. Phys. Chem.* **60**, 241 (2009).  
[6] T. Ritz, P. Thalau, J. B. Phillips, R. Wiltschko, and W. Wiltschko, *Nature (London)* **429**, 177 (2004).  
[7] J. C. Brookes, F. Hartoutsiou, A. P. Horsfield, and A. M. Stoneham, *Phys. Rev. Lett.* **98**, 038101 (2007).  
[8] M. Mohseni, P. Rebentrost, S. Lloyd, and A. Aspuru-Guzik, *J. Chem. Phys.* **129**, 174106 (2008).  
[9] P. Rebentrost, M. Mohseni, I. Kassal, S. Lloyd, and A. Aspuru-Guzik, *New J. Phys.* **11**, 033003 (2009).  
[10] M. B. Plenio and S. F. Huelga, *New J. Phys.* **10**, 113019 (2008).  
[11] F. Caruso, A. W. Chin, A. Datta, S. F. Huelga, and M. B. Plenio, *J. Chem. Phys.* **131**, 105106 (2009).  
[12] K. Maeda, K. B. Henbest, F. Cintolesi, I. Kuprov, C. T. Rodgers, P. A. Liddell, D. Gust, C. R. Timmel, and P. J. Hore, *Nature (London)* **453**, 387 (2008).  
[13] I. K. Kominis, e-print [arXiv:0804.2646](https://arxiv.org/abs/0804.2646).  
[14] J. Cai, G. G. Guerreschi, and H. J. Briegel, *Phys. Rev. Lett.* **104**, 220502 (2010).  
[15] J. Adolphs and T. Renger, *Biophys. J.* **91**, 2778 (2006).  
[16] M. M. Wilde, J. M. McCracken, and A. Mizel, *Proc. R. Soc. London, Ser. A* **466**, 1347 (2010).  
[17] M. Sarovar, A. Ishizaki, G. R. Fleming, and K. B. Whaley, *Nature Phys.* **6**, 462 (2010).  
[18] F. Caruso, A. W. Chin, A. Datta, S. F. Huelga, and M. B. Plenio, *Phys. Rev. A* **81**, 062346 (2010).  
[19] R. Horodecki, P. Horodecki, M. Horodecki, and K. Horodecki, *Rev. Mod. Phys.* **81**, 865 (2009).  
[20] A. J. Leggett and A. Garg, *Phys. Rev. Lett.* **54**, 857 (1985).  
[21] M. Horodecki, P. Horodecki, and R. Horodecki, *Phys. Lett. A* **223**, 1 (1996).  
[22] A. Peres, *Phys. Rev. Lett.* **77**, 1413 (1996).  
[23] V. Vedral and M. B. Plenio, *Phys. Rev. A* **57**, 1619 (1998).  
[24] A. Ishizaki and G. R. Fleming, *Proc. Natl. Acad. Sci. USA* **106**, 17255 (2009).  
[25] S. Hill and W. K. Wootters, *Phys. Rev. Lett.* **78**, 5022 (1997).  
[26] M. B. Plenio, *Phys. Rev. Lett.* **95**, 090503 (2005).  
[27] R. F. Werner, *Phys. Rev. A* **40**, 4277 (1989).  
[28] L. Henderson and V. Vedral, *J. Phys. A* **34**, 6899 (2001).  
[29] H. Ollivier and W. H. Zurek, *Phys. Rev. Lett.* **88**, 017901 (2001).  
[30] J. S. Bell, *Physics (Long Island City, NY)* **1**, 195 (1964).  
[31] T. Werlang, S. Souza, F. F. Fanchini, and C. J. Villas Boas, *Phys. Rev. A* **80**, 024103 (2009).  
[32] A. Datta, A. Shaji, and C. M. Caves, *Phys. Rev. Lett.* **100**, 050502 (2008).  
[33] B. P. Lanyon, M. Barbieri, M. P. Almeida, and A. G. White, *Phys. Rev. Lett.* **101**, 200501 (2008).  
[34] P. W. Shor and S. Jordan, *Quantum Inf. Comput.* **8**, 681 (2008).  
[35] S. Hoyer, M. Sarovar, and K. B. Whaley, *New J. Phys.* **12**, 065041 (2010).  
[36] V. Vedral, *Rev. Mod. Phys.* **74**, 197 (2002).  
[37] R. E. Fenna and B. W. Matthews, *Nature (London)* **258**, 573 (1975).  
[38] F. L. Semião, K. Furuya, and G. J. Milburn, *New J. Phys.* **12**, 083033 (2010).  
[39] A. Olaya-Castro, C. F. Lee, F. F. Olsen, and N. F. Johnson, *Phys. Rev. B* **78**, 085115 (2008).  
[40] T. G. Owens, S. P. Webb, L. Mets, R. S. Alberte, and G. R. Fleming, *Proc. Natl. Acad. Sci. USA* **84**, 1532 (1987).  
[41] A. W. Chin, A. Datta, F. Caruso, S. F. Huelga, and M. B. Plenio, *New J. Phys.* **12**, 065002 (2010).  
[42] P. Rebentrost, R. Chakraborty, and A. Aspuru-Guzik, *J. Chem. Phys.* **131**, 184102 (2009).  
[43] J. Wen, H. Zhang, M. L. Gross, and R. E. Blankenship, *Proc. Natl. Acad. Sci. USA* **106**, 6134 (2009).  
[44] J. D. Whitfield, C. A. Rodríguez-Rosario, and A. Aspuru-Guzik, *Phys. Rev. A* **81**, 022323 (2010).  
[45] B. Schumacher, *Phys. Rev. A* **51**, 2738 (1995).

- [46] B. Groisman, S. Popescu, and A. Winter, [Phys. Rev. A \*\*72\*\*, 032317 \(2005\)](#).
- [47] B. Schumacher and M. D. Westmoreland, [Phys. Rev. A \*\*74\*\*, 042305 \(2006\)](#).
- [48] C. H. Bennett, P. W. Shor, J. A. Smolin, and A. V. Thapliyal, [Phys. Rev. Lett. \*\*83\*\*, 3081 \(1999\)](#).
- [49] C. H. Bennett, P. W. Shor, J. A. Smolin, and A. V. Thapliyal, [IEEE Trans. Inf. Theory \*\*48\*\*, 2637 \(2002\)](#).
- [50] P. W. Shor, in *Quantum Information, Statistics, Probability (Dedicated to A. S. Holevo on the Occasion of his 60th Birthday)* (Rinton Press, Princeton, NJ, 2004), pp. 144–152.
- [51] K. Brádler, P. Hayden, and P. Panangaden, [J. High Energy Phys. \*\*08\*\* \(2009\) 074](#).
- [52] I. Devetak and A. Winter, [IEEE Trans. Inf. Theory \*\*50\*\*, 3138 \(2003\)](#).
- [53] A. Datta, Ph.D. thesis, University of New Mexico, 2008.
- [54] M. A. Nielsen and I. L. Chuang, *Quantum Computation and Quantum Information* (Cambridge University Press, Cambridge, 2000).
- [55] W. H. Zurek, [Phys. Rev. A \*\*67\*\*, 012320 \(2003\)](#).
- [56] T. Kato, *Perturbation Theory for Linear Operators* (Springer, Berlin, 1995).